A Model of Neuronal Bursting Using Three Coupled First Order Differential Equations
Author(s): J. L. Hindmarsh and R. M. Rose
Source: *Proceedings of the Royal Society of London. Series B, Biological Sciences*, Vol. 221, No. 1222 (Mar. 22, 1984), pp. 87-102
Published by: The Royal Society
Stable URL: http://www.jstor.org/stable/35900
Accessed: 28/02/2011 17:40

*Proc. R. Soc. Lond.* B **221**, 87–102 (1984)
*Printed in Great Britain*

# A model of neuronal bursting using three coupled first order differential equations

By J. L. Hindmarsh[1] and R. M. Rose[2]

[1] *Department of Applied Mathematics and Astronomy and* [2] *Department of Physiology, University College, Cardiff, CF*1 1*XL, U.K.*

(*Communicated by Sir Andrew Huxley, P.R.S. – Received* 22 *September* 1983).

We describe a modification to our recent model of the action potential which introduces two additional equilibrium points. By using stability analysis we show that one of these equilibrium points is a saddle point from which there are two separatrices which divide the phase plane into two regions. In one region all phase paths approach a limit cycle and in the other all phase paths approach a stable equilibrium point. A consequence of this is that a short depolarizing current pulse will change an initially silent model neuron into one that fires repetitively. Addition of a third equation limits this firing to either an isolated burst or a depolarizing afterpotential. When steady depolarizing current was applied to this model it resulted in periodic bursting. The equations, which were initially developed to explain isolated triggered bursts, therefore provide one of the simplest models of the more general phenomenon of oscillatory burst discharge.

## Introduction

We have recently described a two variable model of the action potential (Hindmarsh & Rose 1982*a*) which is a modification of Fitzhugh's B.v.P. (Bonhoeffer–van der Pol) model (Fitzhugh 1961), with the property that each action potential is separated by a long interspike interval typical of real neurons. In the phase plane this property results from the close proximity of the nullclines in the subthreshold region of the oscillation. In this paper we examine how this proximity can be exploited to give a qualitative explanation of burst generation. In view of the importance of this proximity for our model, and the way that the phase paths are apparently channelled between the nullclines when they are close together, we refer to this as the narrow channel property. Most of our attention will be directed to molluscan burst neurons, which have been used extensively to investigate the ionic basis of burst activity (Gola 1974; Plant & Kim 1976; Gorman & Hermann 1982).

This work was initiated by the discovery of a cell in the brain of the pond snail *Lymnaea* which was initially silent, but when depolarized by a short current pulse, generated a burst that greatly outlasted the stimulus. Thompson & Smith (1976) have observed a similar type of response in various molluscan burst neurons which had been hyperpolarized to stop the bursting. When these continually hyperpolarized cells were depolarized by a short current pulse they generated an action potential followed by a slow depolarizing after-potential (d.a.p.). Burst discharges triggered by depolarizing current pulses have also been reported in

crustaceans (Russell & Hartline 1982; Dickenson & Nagy 1983), and vertebrates (Schwindt & Crill 1980).

In seeking an explanation for these phenomena we realized that a *small* deformation of the narrow channel in our model would create two additional equilibrium points, and that the resulting three equilibrium point model would have both a stable equilibrium point and a stable limit cycle. The transition from the stable equilibrium point, or silent state, to the stable limit cycle, or repetitively firing state, could be triggered by a short current pulse. Introduction of a third and slower differential equation to represent adaptation was found to terminate this discharge producing either an isolated burst or a d.a.p., depending on the choice of parameters. Application of a steady depolarizing current to this model was then found to produce periodic bursting. In the phase plane these bursts could be seen to be generated by the movement of one of the nullclines between a position with one equilibrium point and a position with three equilibrium points.

Plant & Kim (1976) have discussed a model of bursting which is an extension of the Hodgkin–Huxley model (Hodgkin & Huxley 1952), and uses seven coupled first order differential equations. The model described here retains the main features of Plant & Kim's model (see Discussion) but is simpler with bursting explained using a two dimensional phase plane. This has the advantage of making it easier to understand interactions between bursting neurons (R. M. Rose and J. L. Hindmarsh, unpublished).

The equations may be seen as a mathematical representation of bursting properties in terms of a B.v.P. type of model (Fitzhugh 1961), this representation being qualitative and dependent on the narrow channel property of our original equations (Hindmarsh & Rose 1982*a*).

## The three equilibrium point model

Consider the following system of differential equations as a model for the action potential

$$\dot{v} = \alpha(\beta r - f(v) + I) \tag{1}$$

$$\dot{r} = \gamma(g(v) - \delta r), \tag{2}$$

in which $v$ represents membrane potential, $r$ is a recovery variable, $I$ is applied current, and $\alpha$, $\beta$, $\gamma$ and $\delta$ are constants. These equations generalize Fitzhugh's B.v.P. model (Fitzhugh 1961) and our modification of that model (Hindmarsh & Rose 1982*a*). In these equations we could set $\alpha = 1/C$ where $C$ is the membrane capacity and also set $\beta = 1$ without loss of generality. However we will shortly simplify these equations by defining new variables. The form of the functions $f(v)$ and $g(v)$ in (1) and (2) may be determined partly by voltage clamp experiments in which the initial ($\mathrm{I}_{v_\mathrm{p}}(0)$) and steady-state ($I_{v_\mathrm{p}}(\infty)$) values of clamping current are measured for a range of clamping voltages ($v_\mathrm{p}$), and partly by the requirement that $f(v)$ be cubic (see Hindmarsh & Rose 1982*a*, *b*).

Then $f(v_\mathrm{p}) = I_{v_\mathrm{p}}(0)$, and $g(v_\mathrm{p}) = f(v_\mathrm{p}) - I_{v_\mathrm{p}}(\infty)$ (Hindmarsh & Rose 1982*a*). In both Fitzhugh's and our model, the function $f(v)$ is a cubic, but Fitzhugh (1961) assumed that $g(v)$ was linear, whereas we calculated $g(v)$ using an $I(\infty)$ curve

similar to that shown in figure 1*a*. As a result, in the phase plane representation of these equations our model is different from that of Fitzhugh in that $v$ and $r$ nullclines, the curves labelled $\dot{v} = 0$ and $\dot{r} = 0$ in figure 1*b* lie close together for $v < 0$, and consequently the phase point moves slowly along the narrow channel between the nullclines giving a long interspike interval (Hindmarsh & Rose 1982*a*). Also the phase plane for this model, shown schematically in figure 1*b*, has only one equilibrium point given by the intersection of the $v$ and $r$ nullclines. In a repetitively firing cell this equilibrium point is unstable.

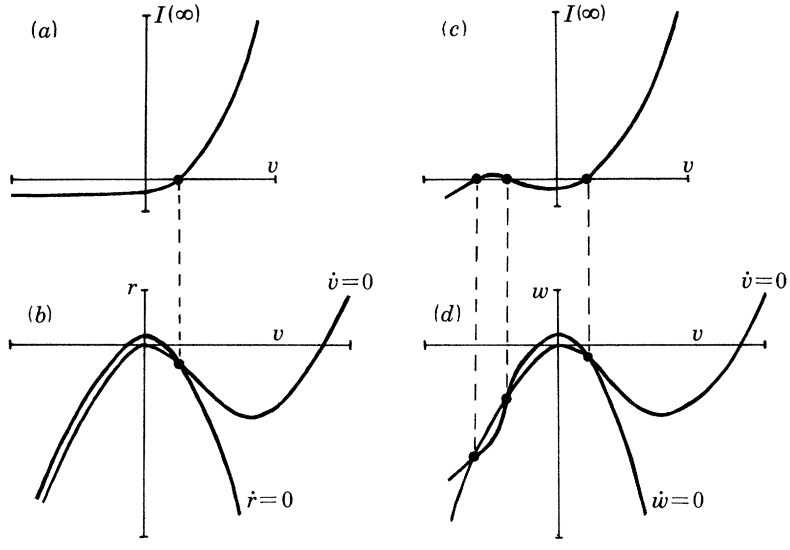


FIGURE 1. Schematic illustration of steady state current–voltage ($I(\infty)-v$) curves (*a*) for the one equilibrium point model, and (*c*) for the three equilibrium point model, and the corresponding $v$ and $r$ nullclines in the phase plane, (*b*), and $v$ and $w$ nullclines in the phase plane, (*d*).

The main aim of this paper is to discuss a further modification to the model which is illustrated in figure 1*c*, *d*. If the $I(\infty)$ curve is deformed *slightly* so that it has three intersection points with the $I(\infty) = 0$ axis, then this change creates three equilibrium points in the phase plane. Physiologically this modification would correspond to the addition of a slow inward current whose time constant is similar to that of the recovery ($r$) process in the model. If this inward current were described by an equation of the form:

$$\dot{z} = \gamma(h(v) - \delta z) \tag{3}$$

then, defining a new variable $w = r + z$, we obtain

$$\dot{w} = \gamma(g(v) + h(v) - \delta w) \tag{4}$$

which is of the same form as (2).

The assumption of equal time constants is probably inaccurate, since we estimate from data on R15 of *Aplysia* (Gola 1974; Plant & Kim 1976) that the slow inward current may be five to ten times slower than the outward potassium

current. However as shown later the assumption may be more appropriate for bursting cells that switch on more rapidly than R15, in which case it may be a reasonable simplification which does not greatly alter the qualitative behaviour.

A simple form of the equations for the new model may be arrived at as follows (for the case $I = 0$). First transform (1) and (4) by defining a new time variable $T = \gamma\delta t$ and introducing new variables $x$ and $y$ defined by:

$$x(T) = v(T), \quad y(T) = \frac{\alpha\beta}{\gamma\delta} w(t)$$

which satisfy the differential equations

$$\dot{x} = y - F(x) \tag{5}$$

$$\dot{y} = G(x) - y \tag{6}$$

where

$$F(x) = \frac{\alpha}{\gamma\delta} f(x) \quad \text{and} \quad G(x) = \frac{\alpha\beta}{\gamma\delta^2}(g(x) + h(x)).$$

In these equations $x$ is the membrane potential and $y$ the recovery variable as in Fitzhugh's B.v.P model (Fitzhugh 1961) and our earlier model (Hindmarsh & Rose 1982*a*). Now impose the following conditions on $F(x)$ and $G(x)$:

(i) $F(x)$ is a cubic (and $F(x) \to \infty$ as $x \to \infty$);

(ii) $G(x)$ is quadratic;

(iii) $F(x)$ and $G(x)$ both have a local maximum for the same value of $x$.

Condition (i) follows from Fitzhugh (1961) and Hindmarsh & Rose (1982*a*). Condition (ii) is a simplification of our earlier (experimental) form for $G(x)$ (Hindmarsh & Rose 1982*a*), and condition (iii) is an approximation in the interests of simplicity. Finally we choose the origin of the $x$–$y$ plane so that $F(x)$ and $G(x)$ have their local maximum at $x = 0$, and that the value of $F(x)$ at $x = 0$ is zero. With these conditions the general form of $F(x)$ and $G(x)$ is:

$$F(x) = ax^3 - bx^2,$$

and

$$G(x) = c - dx^2 \quad (a, b, c, d > 0).$$

giving the following equations

$$\dot{x} = P(x, y) \equiv y - ax^3 + bx^2, \tag{7}$$

$$\dot{y} = Q(x, y) \equiv c - dx^2 - y \tag{8}$$

The only difference between these equations and the Fitzhugh B.v.P. model (Fitzhugh 1961) is that the $y$ nullcline is now parabolic instead of a straight line.

## Properties of the model

### (*a*) *Equilibrium points*

The equilibrium points (e.p.s) are given by the intersection of the $x$ and $y$ nullclines, where $P(x, y) = 0 = Q(x, y)$. Eliminating $y$, the $x$ coordinates of the equilibrium points are given by the roots of $F(x) = G(x)$ or

$$x^3 + px^2 = q, \tag{9}$$

where

$$p = \frac{d-b}{a} \quad \text{and} \quad q = \frac{c}{a}.$$

Now $q > 0$ since $a > 0$ and $c > 0$. Therefore there will be one e.p. if $p < 0$, giving nullclines similar to those of figure 1*b*. The condition for three e.p.s. is that $27\,q < 4p^3$, or that $27\,a^2 c < 4\,(d-b)^3$, which in turn requires that $b < d$.

TABLE 1. ($D = (b^2-3a)^{\frac{1}{2}}$, $b^2 > 3a$)

| region | values of $x_0$ | sign of $\mathrm{Tr}(A(x_0))$ | sign of $\mathrm{Det}(A(x_0))$ | type of e.p. |
|---|---|---|---|---|
| I | $x_0 < -2(d-b)/3a$ | − | + | stable node or spiral |
| II | $-2(d-b)/3a < x_0 < 0$ | − | − | unstable saddle |
| III | $0 < x_0 < (b-D)/3a$ | − | + | stable focus or spiral |
| IV | $(b-D)/3a < x_0 < (b+D)/3a$ | + | + | unstable focus or spiral |
| V | $(b+D)/3a < x_0$ | − | + | stable focus or spiral |

### (*b*) *Stability*

The stability of these e.p.s may be investigated using the linear approximations to (7) and (8) (Arrowsmith & Place (1982), chapter 3). At the e.p. whose $x$-coordinate is $x_0$ the linear approximation is:

$$\begin{bmatrix} \dot{u}_1 \\ \dot{u}_2 \end{bmatrix} = A(x_0) \begin{bmatrix} u_1 \\ u_2 \end{bmatrix},$$

where $u_1$ and $u_2$ are new coordinates whose origin is at the e.p. and

$$A(x_0) = \begin{bmatrix} \dfrac{\partial P}{\partial x}, & \dfrac{\partial P}{\partial y} \\ \dfrac{\partial Q}{\partial x}, & \dfrac{\partial Q}{\partial y} \end{bmatrix}_{(x_0, y_0)} = \begin{bmatrix} -3\,ax_0^2 + 2\,bx_0, & 1 \\ -2\,dx_0, & -1 \end{bmatrix}$$

The type of e.p. is determined by the signs of the trace and determinant of $A(x_0)$. The trace and determinant are given by:

$$\mathrm{Tr}\,(A(x_0)) = -3ax_0^2 + 2bx_0 - 1,$$
$$\mathrm{Det}\,(A(x_0)) = 3ax_0^2 + 2(d-b)\,x_0.$$

Now provided $b^2 > 3a$, $\mathrm{Tr}\,(A(x_0))$ is negative for all values of $x_0$ except those between $(b-(b^2-3a)^{\frac{1}{2}})/3a$ and $(b+(b^2-3a)^{\frac{1}{2}})/3a$. $\mathrm{Det}(A(x_0))$ is positive for all values of $x_0$ except those between $-2(d-b)/3a$ and 0. Thus we may divide the $x$-axis into five regions according to the signs of $\mathrm{Tr}\,(A(x_0))$ and $\mathrm{Det}\,(A(x_0))$. Table 1 gives the type of e.p. according to the region to which $x_0$ belongs.

If $b^2 < 3a$ then $\mathrm{Tr}\,(A(x_0))$ is negative for all values of $x_0$, and the only possible types of e.p. are unstable saddle or stable focus or spiral. This precludes the possibility of an unstable focus or spiral whose phase paths approach a stable limit

cycle. Since we want this to be our model of the repetitively firing cell we impose the condition that $b^2 > 3a$.

### (*c*) *Location of roots*

The Poincaré Index (Jordan & Smith (1977), chapter 3) of the single e.p. in the phase plane of figure 1*b* is 1. The introduction of two additional e.p.s as in figure 1*d* does not change the sum of the indices of all the e.p.s and it is easily seen that the leftmost and rightmost e.p.s have index 1, while the middle e.p. has index $-1$. Thus the middle e.p. corresponds to a saddle point and must have its $x$-coordinate in region II. It follows that the leftmost e.p. must have its $x$-coordinate in region I and so be a stable node or spiral. This leaves open the question of the location of the $x$-coordinate of the rightmost e.p. As remarked above, we obtain a simple model of a repetitively firing cell if this e.p. is an unstable node or spiral. So we require the $x$-coordinate of the rightmost e.p. to lie in region IV.

The lower and upper boundaries of region IV are given by:

$$L = \frac{b-D}{3a}, \tag{10}$$

and

$$M = \frac{b+D}{3a}, \tag{11}$$

respectively. If $L^3+pL^2 = q$ then the positive root of the cubic (9) will be $L$, and if $M^3+pM^2 = q$ it will be $M$. So provided

$$L^3+pL^2 < q < M^3+pM^2, \tag{12}$$

the positive root will lie in region IV.

The conditions (10) and (11) are shown graphically in figure 2. There the roots of the cubic (9) are the $x$-coordinates of the points of intersection of the graph of $x^3+px^2$ with the horizontal line of height $q$ above the $x$-axis. To have three roots, represented by the points $A$, $B$ and $C$, we must have $0 < 27q < 4p^3$, and the instability condition on the e.p. corresponding to the positive root is $L < C < M$ which can also be expressed by (12).

### (*d*) *Numerical solution*

An example of the type of response that we wish to simulate is shown in figure 3*b*, which is an intracellular recording from a small identified cell in the visceral ganglion of the pond snail *Lymnaea*. The cell is usually silent, but when depolarized for about 100 ms it fires several times, and continues to fire after cessation of the stimulating current. Adding to (7) a term $I$, to represent the external current, we obtain:

$$\dot{x} = y-ax^3+bx^2+I, \tag{13}$$

$$\dot{y} = c-dx^2-y. \tag{14}$$

A numerical solution to (13) and (14) for a short current pulse ($I$) is shown in figure 3*a*. During the application of the current pulse the $x$ value rises steadily, and as in the real neuron the model discharges repetitively after termination of the current

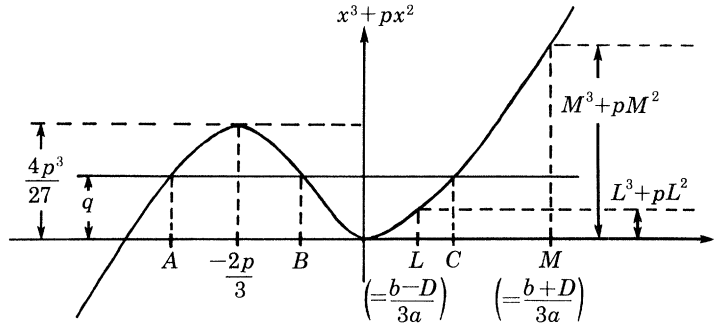


FIGURE 2. Location of roots of the equation $x^3+px^2 = q$. Explanation in text.

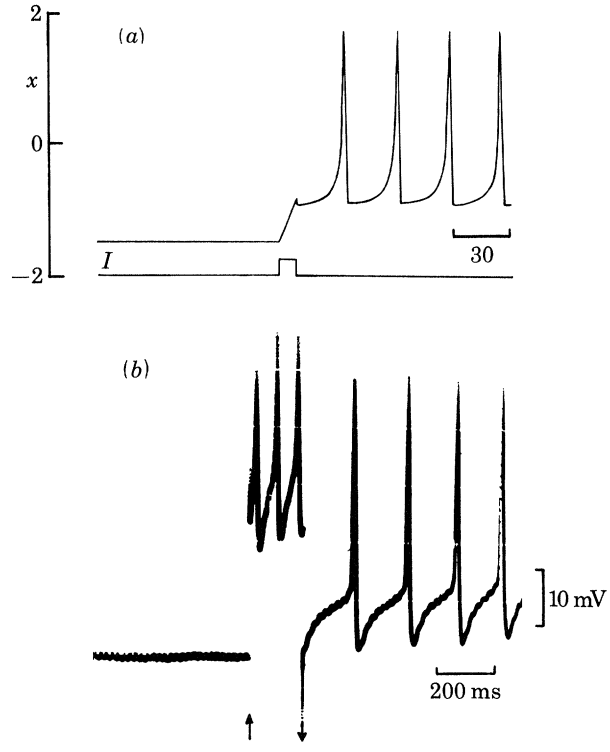


FIGURE 3. Triggered repetitive firing. (*a*) Numerical solution to (13) and (14) with $a = 1$, $b = 3$, $c = 1$, $d = 5$, for a short current pulse ($I = 1$). (*b*) Intracellularly recorded response of a small identified cell in the visceral ganglion of the snail *Lymnaea stagnalis*, for a short depolarizing current pulse applied between arrows. Upward displacement of baseline during current pulse is due to bridge imbalance.

pulse. One difference between the model and the cell is that it is always necessary to fire the cell several times during application of the current pulse for an afterdischarge to occur. In the model it is possible to produce the afterdischarge by the application of a shorter current pulse which does not fire the cell (figure 3*a*). This difference could arise because the subthreshold inward current has slower

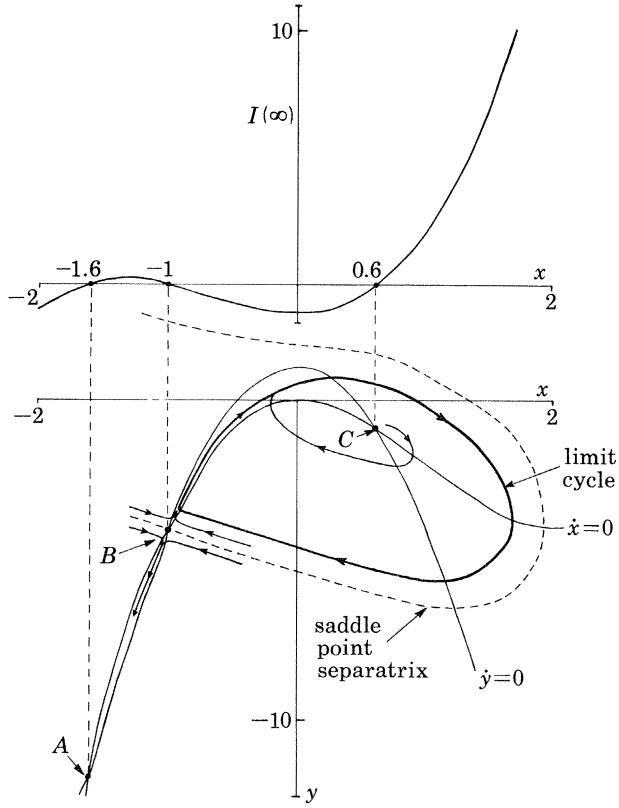


FIGURE 4. Phase plane representation of (7) and (8) with $a = 1$, $b = 3$, $c = 1$, $d = 5$. The equilibrium points (e.p.s) A, B and C are a stable node, an unstable saddle, and an unstable spiral respectively. Corresponding current–voltage ($I(\infty) - x$) curve is shown above phase plane. Explanation in text.

activation kinetics in the snail neuron than is assumed in the model. Also the recorded action potentials have a greater undershoot and more rapid recovery than in the model, although this difference is to be expected because it was present in our original model (Hindmarsh & Rose 1982*a*). The three equilibrium point model therefore shows the property of triggered firing at least qualitatively.

### (*e*) *Phase plane representation*

This property of triggered firing can be understood most easily by examining the behaviour in the phase plane (figure 4). For convenience the calculated solutions in figure 3*a* and 4 were obtained with the constants $a = 1$, $b = 3$, $c = 1$, $d = 5$, so that the equilibrium points are easily located at $x$ values of $-1.6$, $-1$ and $+0.6$. As predicted by the analysis (table 1) the leftmost equilibrium point is a stable node, the middle equilibrium point is a saddle point, and the rightmost equilibrium point is an unstable spiral. If the initial conditions for $x$ and $y$ are chosen to be close to the unstable equilibrium point on the right, the phase point spirals out until it enters a limit cycle. On the other hand if the point is started close to the

saddle point and the direction of integration reversed, we obtain the dashed line that divides the phase plane into two regions. On one side of this line the phase point joins the limit cycle, whereas on the other side it is deflected downwards towards the stable node. The phase plane isoclines are related to the steady-state current–voltage curve shown above the diagram, with the $x$-coordinates of the equilibrium points A, B and C given by the $x$-coordinates of the points where $I(\infty) = 0$. This current–voltage curve is similar to that proposed to underlie triggered discharges in cat motoneurons in the presence of penicillin (Schwindt & Crill 1980), and to the current–voltage curve obtained for molluscan burst cells such as R15 of *Aplysia* under voltage clamp (Gola 1974).

In the calculated response to a current step, the model was initially in equilibrium at $x = -1.6$. On application of the current step, the $\dot{x} = 0$ isocline was displaced downwards, eliminating the two equilibrium points on the left hand side of the phase plane. Therefore the phase point moved fairly rapidly upwards and to the right, giving the fall in membrane potential observed in figure 3*a*. On termination of the current step, the $\dot{x} = 0$ isocline moves back to the original position, recreating the two equilibrium points on the left hand side. If the phase point is below the saddle point when this happens, it moves slowly back to the leftmost equilibrium point. On the other hand if the phase point is above the saddle point on termination of the current pulse, it enters the limit cycle and an infinite train of impulses result (figure 3*a*). It can therefore be seen that triggered firing results because the model is changed temporarily from a three equilibrium point model to one having a single unstable equilibrium point during the application of the current pulse.

## Addition of a third differential equation

### (*a*) *Adaptation*

The cell in *Lymnaea* which has been discussed earlier did not fire indefinitely, but slowed down and terminated with a slow after-hyperpolarizing wave (figure 5*b*). A simple way of producing this effect would seem to be the introduction of a slow current, which gradually hyperpolarizes the cell. A slowly increasing outward current has been reported to cause adaptation in molluscan neurons (Partridge & Stevens 1976), and is generally assumed to underlie the repolarization process in molluscan bursters (Plant & Kim 1976; Gorman & Hermann 1982). In the following system of equations we have added an adaptation current ($z$) to (13). This adaptation current approaches a steady-state value, which we assume to be a linear function of $x$. Other authors have represented adaptation as a conductance variable with a sigmoidal steady-state curve (Colding-Jørgensen 1976) to be consistent with the Hodgkin–Huxley formulation (Hodgkin & Huxley 1952). Our equations are closer to Fitzhugh's model (Fitzhugh 1961) in that the $\dot{x}$, $\dot{y}$ and $\dot{z}$ equations have cubic, quadratic, and linear terms in $x$ respectively. The equations for the three equilibrium point model with adaptation are:

$$\left.\begin{aligned} \dot{x} &= y - ax^3 + bx^2 + I - z, \\ \dot{y} &= c - dx^2 - y, \\ \dot{z} &= r(s(x - x_1) - z), \end{aligned}\right\} \tag{15}$$

where $(x_1, y_1)$ are the coordinates of the leftmost e.p. of the model without adaptation. This has the result that $(x_1, y_1, 0)$ is a stable e.p. of the model with adaptation. For numerical investigation we will use $a = 1$, $b = 3$, $c = 1$ and $d = 5$ as previously.

The responses of this model to a short depolarizing current pulse depend on the values given to the constants $r$ and $s$. For the case $r = 0.001$, $s = 1$, an isolated

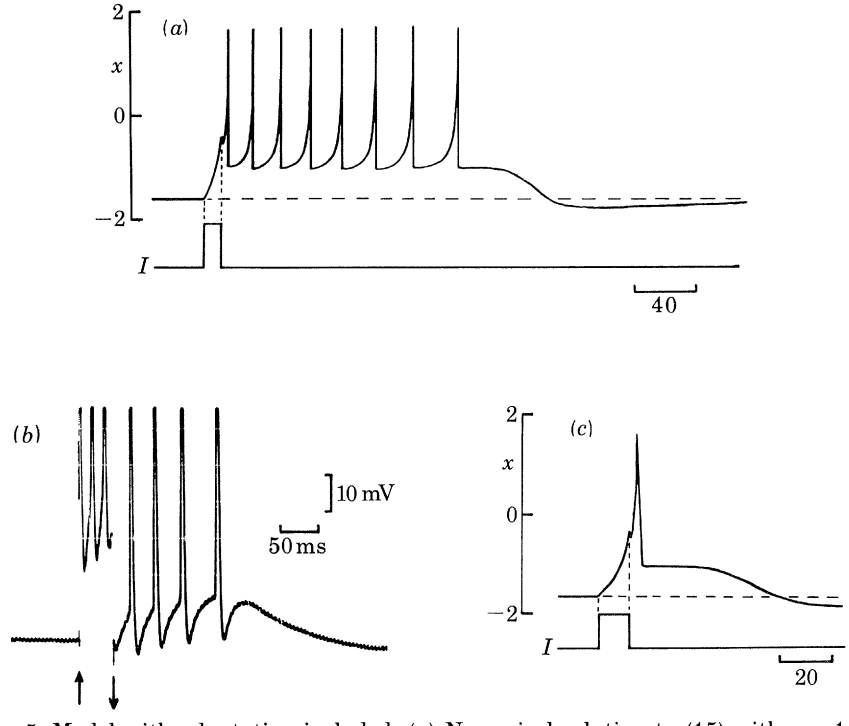


FIGURE 5. Model with adaptation included. (*a*) Numerical solution to (15) with $a = 1$, $b = 3$, $c = 1$, $d = 5$, $r = 0.001$, $s = 1$, for a short current pulse ($I = 1$), showing a triggered burst; (*b*) example of a triggered burst recorded intracellularly from the identified cell in the *Lymnaea* visceral ganglion; (*c*) numerical solution as in (*a*) but with $s = 4$, showing a depolarizing afterpotential.

burst of action potentials is obtained (figure 5*a*) similar to that obtained experimentally in *Lymnaea* (figure 5*b*). For $r = 0.001$, $s = 4$, the response shown in figure 5*c* is obtained, which is similar to the d.a.p.s observed by Thompson & Smith (1976). One difference between calculated and recorded waveforms is that the recorded d.a.p.s are biphasic with an initial dip before rising to a peak (Thompson & Smith 1976). Similarly, recorded bursts tend to have an initial acceleration before adaptation takes place (figure 5*b*). These features are not shown by the model, which gives steadily declining afterpotentials (figure 5*c*) or spike frequencies (figure 5*a*).

One feature that is interesting is that after the burst the model slowly hyperpolarizes to an $x$ value that is more negative than the starting value $(x_1)$. When this hyperpolarization is complete we have found that the $x$ value returns very slowly to the original value $x_1$ (see also figure 6*a*).

We can understand these effects by considering what happens in the $x$–$y$ phase plane. Strictly speaking, since there are three variables, $x$, $y$ and $z$, we should be looking at a three dimensional phase space. However, the third variable $z$ is slowly varying ($r = 0.001$) compared to $x$ and $y$. We therefore regard $z$ as a slowly varying parameter in the equations for $\dot{x}$ and $\dot{y}$.

Consider the model neuron, initially at rest at $x_1$, which is given a short current step. As before (figure 4) the phase point will enter a limit cycle, but now each time an action potential occurs the adaptation current ($z$) will be incremented, and this will displace the $x$ nullcline upwards on successive cycles. The firing frequency will decrease because the narrow channel on the left hand side of the phase plane (figure 4) becomes narrower. Also as the $x$ nullcline is displaced upwards the equilibrium points will move, the saddle point being displaced upwards and the leftmost equilibrium point being displaced downwards. Eventually the saddle point will be displaced upwards so far that the limit cycle trajectory will cross the saddle point separatrix (figure 4). Thus the firing ceases and the phase point enters the narrow channel below the saddle point and moves slowly downwards towards the leftmost equilibrium point. This slow movement gives rise to the slow hyperpolarizing wave, which approaches a value below $x_1$ because the leftmost equilibrium point has been displaced downwards. As the adaptation current relaxes back to its starting value, the $x$ value will reapproach $x_1$ as the leftmost equilibrium point moves back to its original position.

### (*b*) *Burst generation*

As remarked in the Introduction, Thompson & Smith (1976) converted bursting cells into cells that produced d.a.p.s in response to current pulses, by the introduction of a constant hyperpolarizing current. Conversely we expect our equations to model a bursting cell when the current parameter ($I$) is set at a constant positive level. Numerical solutions for different values of applied current ($I$), but without further modification to the other parameters are shown in figure 6. At low levels of steady depolarizing current ($I = 0.4$, figure 6*a*), the model generated an isolated burst followed by an after-hyperpolarizing wave which slowly recovered to the starting value ($x_1$). At higher levels of current ($I = 2$) the model generated a long burst initially in response to the current step, and this adapted and terminated to give the periodic burst pattern shown in figure 6*b*. These bursts are similar to the bursts of cell R15 of *Aplysia* (Gola 1974) except that the model switches on and off more rapidly presumably because our equivalent of the slow inward current has a faster time constant than in the real cell. At still higher levels of current ($I = 4$) there was a continuous high frequency discharge, with the frequency declining from the onset of the step to the steady repetitive firing shown in figure 6*c*.

Again burst generation can be easily understood by use of the $x$–$y$ phase plane (figure 7). The phase plane will be examined at five points ($\alpha$–$\varepsilon$) on the burst cycle shown schematically in figure 7*a*. At $\alpha$ the adaptation current is just beginning to rise and the applied current ($I$) has changed the three equilibrium point model to one having a single unstable equilibrium point (figure 7*b*) by downward displacement of the $x$ nullcline. Consequently the model generates a burst of action

potentials because of the presence of the limit cycle. As the adaptation current rises the $x$ nullcline moves upwards and a saddle point is created which moves slowly upwards as the adaptation current continues to rise. Eventually the phase point is displaced across the saddle point separatrix, and enters the narrow channel below the saddle point and the burst switches off (figure 7*c*). This process is identical to

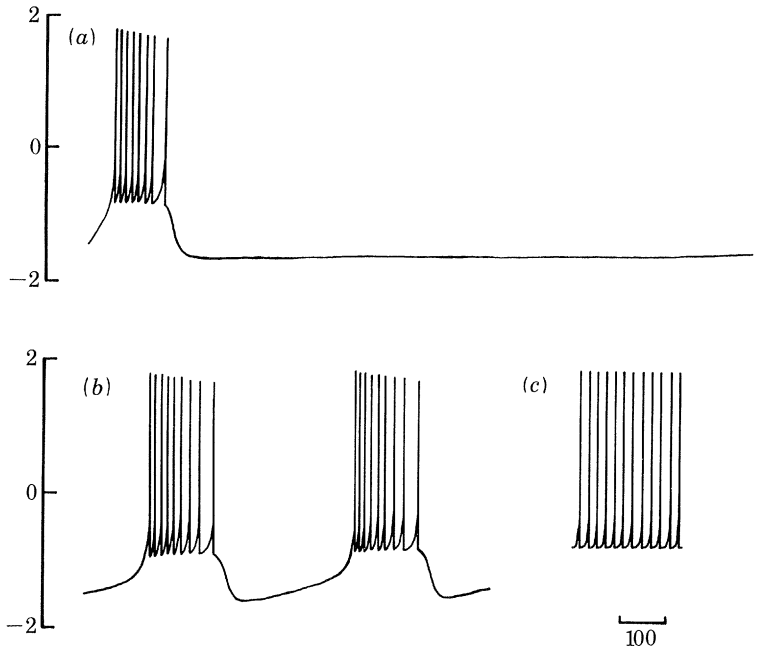


FIGURE 6. Burst generation. Numerical solution of (15) with $a = 1, b = 3, c = 1, d = 5, r = 0.001$, $s = 4$, for (*a*) $I = 0.4$, (*b*) $I = 2$, (*c*) $I = 4$; (*b*) starts 700 time units after the onset of $I$ step, and (*c*) after 1000 time units of continuous firing.

that described in the previous section on isolated burst generation. At point β the phase point is moving down the narrow channel towards the leftmost equilibrium point (figure 7*c*). When the post-burst hyperpolarization is completed the phase point has reached the leftmost equilibrium point. The adaptation current then starts to fall, displacing the $x$ nullcline downwards again. As this happens the leftmost equilibrium point and the saddle point approach each other (figure 7*d*), the slow upward movement of the lower equilibrium point causing the inter-burst pacemaker depolarization at point γ. At point δ the two equilibrium points coalesce (figure 7*e*) and finally at ε the model switches back to a one equilibrium point model which has the phase plane shown in figure 7*f* and figure 7*b*, so that another burst is generated. Burst generation therefore arises through a regular alternation between one and three equilibrium point states.

### (*c*) *Random burst structure*

With parameter values $a = 1$, $b = 3$, $c = 1$, $d = 5$, $r = 0.005$, $s = 4$ and current $I = 3.25$ the numbers of spikes in successive bursts were 7, 5, 5, 7, 5, 5, 5, 5, 6,

4, 3, 3, 7, 5, 4, 5, 7, without any apparent pattern. Thus we have an example of a deterministic system producing bursts with a random structure. This example shows that a random burst structure does not necessarily require that the system is subject to random forces or noise.

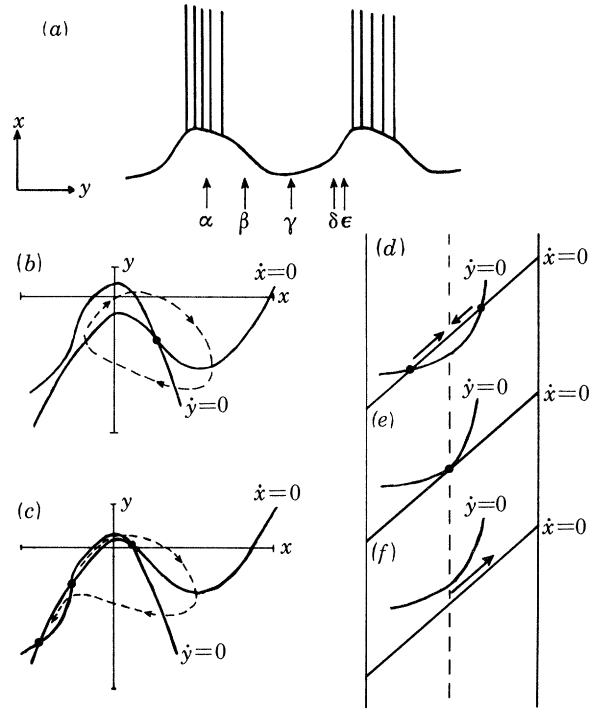


FIGURE 7. (a) Schematic representation of burst cycle; (*b*) and (*c*) are phase plane diagrams corresponding to times α and β; (*d*) to (*e*) show details of the *x*–*y* phase plane diagrams corresponding to times γ to ε in the burst cycle.

### (*d*) *Post-inhibitory rebound*

A further feature of the model that arises without further modification, is that it shows post-inhibitory rebound. If the model is hyperpolarized for a period similar to the burst duration, the adaptation current will decrease below its resting value. Consequently when the hyperpolarizing current is released, the model will behave as though extra current had been applied, and the phase plane will be similar to that in figure 7*b*. The model will generate a post-inhibitory rebound burst, which will terminate in the usual way as the adaptation current rises back to its resting value. An example of this effect using exactly the same parameter values as in figures 5*c* and 6 but with the applied current (*I*) given in the hyperpolarizing direction for a period similar to the burst duration is shown in figure 8.

## Discussion

A current view of burst generation in molluscan neurons, based on voltage clamp experiments, is as follows (Gorman & Hermann 1982). Firstly in the interburst interval the rising depolarization activates a subthreshold inward current carried primarily by $Ca^{2+}$ ions, which initiates the burst. During the burst both the slow depolarization and the action potentials cause $Ca^{2+}$ entry into the cell, which in

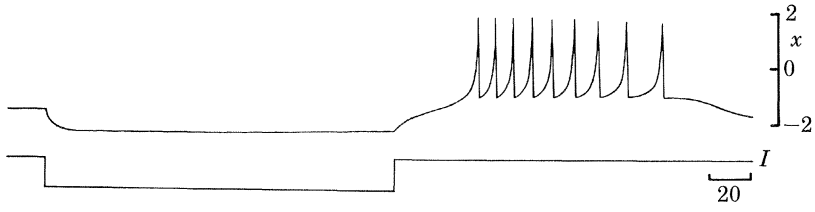


Figure 8. Post-inhibitory rebound. Numerical solution of (15) for a long hyperpolarizing step ($I = -3$). Other parameters as in figures 5*c* and 6.

turn activates a slow outward $Ca^{2+}$ dependent $K^+$ current. This current terminates the cycle causing the post-burst hyperpolarization. The slow outward current then declines and the cell slowly depolarizes to initiate another cycle. This mechanism is broadly consistent with our model. The subthreshold inward current of molluscan burst neurons is known to give rise to a region of negative slope in the $I$–$V$ characteristic in a voltage range and of a magnitude which is qualitatively similar to that in our model (Gola 1974; Smith *et al.* 1975; Wilson & Wachtel 1974). The $Ca^{2+}$ activated $K^+$ current may be thought of as equivalent to our $z$ current.

A mechanism similar to this has been expressed mathematically in a model of bursting given by Plant & Kim (1976). To understand the relationship between their model and ours it is useful to consider both models as a modification to the repetitively firing neuron. The most complete model of repetitive firing in molluscan neurons is that of Connor & Stevens (1971). They added a fast outward current to the Hodgkin–Huxley model (Hodgkin & Huxley 1952) giving a description involving six differential equations. Using this as a starting point, Plant & Kim (1976) included an additional constant inward current and a slowly activated outward current described by a seventh differential equation. Our model is similar to this except that we have started with a model for repetitive firing which uses only two differential equations (Hindmarsh & Rose 1982*a*). The subthreshold inward current has been incorporated by deforming the steady state $I$–$V$ curve without a change in the number of variables, and the slow outward current is included as a third differential equation. Therefore we have modelled essentially the same mechanism as Plant & Kim (1976) using three differential equations instead of seven. The advantage of this is that since one of our variables ($z$) changes slowly, the overall mechanism can be easily represented in the two dimensional phase plane and the stability of the equilibrium points can be analysed. It is therefore easier to understand related phenomena such as triggered bursting and

post-inhibitory rebound. It is for instance possible to predict another type of bursting. If the unstable equilibrium point in region IV is displaced into region III (table 1) before the upwardly displaced saddle point has time to switch off the burst, the phase point will spiral into the stable focus in region III. When the $z$ variable relaxes again, the phase point will spiral out to meet the limit cycle again. This should lead to a burst pattern with spike amplitude increasing and decreasing at the beginning and end of each burst. We have observed this type of bursting in the *Lymnaea* brain (R. M. Rose, unpublished observations).

Although there are other possible mechanisms for the generation of d.a.p.s, for instance recurrent synaptic excitation, extracellular $K^+$ accumulation during activity, and local circuit currents from dendrites, there are strong arguments against these mechanisms at least in the case of molluscan neurons (Thompson & Smith 1976). The latter authors conclude that the dominant mechanism in d.a.p. production is activation of the subthreshold inward current of bursting neurons and its slow inactivation. We have not attempted to include inactivation mechanisms in our model but recognize this as an alternative.

Although there are obvious applications of the model to small oscillatory networks because of the economy of variables, an important problem to be answered is the physical meaning of the $x$, $y$ and $z$ variables. The problem is how to relate our original model to the Hodgkin–Huxley model (Game 1982). Although there are difficulties here, we think that the topological features of the narrow channel and its deformation may survive a considerable amount of modification and reinterpretation. In conclusion, the model, which is a natural extension of Fitzhugh's model of the nerve impulse (Fitzhugh 1961) should be regarded in the same way as a qualitative representation of a further set of neural properties in the phase plane.

We thank Sir Andrew Huxley, P.R.S., for his helpful comments and Dr D. A. Evans for assistance with the numerical work.

## References

Arrowsmith, D. K. & Place, C. M. 1982 *Ordinary differential equations.* London: Chapman & Hall:

Colding-Jørgensen, M. 1976 A description of adaptation in excitable membranes. *J. theor. Biol.* **63**, 61–87.

Connor, J. A. & Stevens, C. F. 1971 Prediction of repetitive firing behaviour from voltage-clamp data on an isolated neurone soma. *J. Physiol., Lond.* **213**, 31–53.

Dickenson, P. S. & Nagy, F. 1983 Control of a central pattern generator by an identified modulatory interneurone in crustacea. II. Induction and modification of plateau properties in pyloric neurones. *J. exp. Biol.* **105**, 59–82.

Fitzhugh, R. 1961 Impulses and physiological states in theoretical models of nerve membrane. *Biophys. J.* **1**, 445–466.

Game, C. J. A. 1982 BVP models of nerve membrane. *Nature, Lond.* **299**, 375.

Gola, M. 1974 Neurones à ondes-salves des mollusques, variations cycliques des conductances ioniques. *European J. Physiol.* **352**, 17–36.

Gorman, A. L. F. & Herman, A. 1982 Quantitative differences in the currents of bursting and beating molluscan pacemaker neurones. *J. Physiol., Lond.* **333**, 681–699.

Hindmarsh, J. L. & Rose, R. M. 1982*a* A model of the nerve impulse using two first order differential equations. *Nature, Lond.* **296**, 162–164.

Hindmarsh, J. L. & Rose, R. M. 1982*b* BVP models of nerve membrane (reply to C. J. A. Game). *Nature, Lond.* **299**, 375.

Hodgkin, A. L. & Huxley, A. F. 1952 A quantitative description of membrane current and its application to conduction and excitation in nerve. *J. Physiol., Lond.* **117**, 500–544.

Jordan, D. W. & Smith, P. 1977 *Nonlinear ordinary differential equations.* Oxford: Clarendon Press.

Partridge, L. D. & Stevens, C. F. 1976 A mechanism for spike frequency adaptation. *J. Physiol., Lond.* **256**, 315–332.

Plant, R. E. & Kim, M. 1976 Mathematical descriptions of a bursting pacemaker neuron by a modification of the Hodgkin–Huxley equations. *Biophys. J.* **16**, 227–244.

Russell, D. F. & Hartline, D. K. 1982 Slow active potentials and bursting motor patterns in pyloric network of the lobster *Panulirus interruptus. J. Neurophysiol.* **48**, 914–937.

Schwindt, P. & Crill, W. 1980 Role of persistent inward current in motoneuron bursting during spinal seizures. *J. Neurophysiol.* **43**, 1296–1317.

Smith, T. G., Barker, J. L. & Gainer, H. 1975 Requirements for bursting pacemaker potential activity in molluscan neurons. *Nature, Lond.* **253**, 450–452.

Thompson, S. H. & Smith, S. J. 1976 Depolarizing afterpotentials and burst production in molluscan pacemaker neurones. *J. Neurophysiol.* **39**, 153–161.

Wilson, W. A. & Wachtel, H. 1974 Negative resistance characteristic essential for the maintenance of slow oscillations in bursting neurones. *Science, N.Y.* **186**, 932–934.